Poster # PO-094

Metabolism regulating metal phenolic networks reverse the immunosuppressive tumor microenvironment

Hoyeon Nam [1], Heewon Park [1], Mi Kwon Son [2], Yuri Choi [1], Yong-kyu Lee [2, 3,*], Yeu-Chun Kim [1,*]

[1] Department of Chemical & Biomolecular Engineering, Korea Advanced Institute of Science and Technology (KAIST), Daejeon, Korea / [2] 4D Convergence Technology Institute (National Key Technology Institute in University), Korea National University of Transportation, Jeungpyeong, Korea / [3] Department of Chemical & Biological Engineering, Korea National university of Transportation, Chungju, Korea

ABSTRACT & INTRODUCTION

- Targeting cancer cell metabolism has emerged as a promising strategy to reverse the immunosuppressive tumor microenvironment (TME).
- Aerobic glycolysis, the dominant metabolic pathway in cancer cells, leads to glucose depletion and the accumulation of immunosuppressive metabolites such as lactate, ultimately limiting the efficacy of conventional immunotherapies.
- To overcome this limitation, a zinc-based metal phenolic-networks (MPNs) were developed by coating zinc oxide (ZnO) nanoparticles with epigallocatechin gallate (EGCG) to modulate cancer metabolism for TME reprogramming and immune activation. Furthermore, severe starvation stress induced by dual metabolic inhibition triggered immunogenic cell death (ICD) without the need for conventional ICD inducers.
- *In vitro* and *in vivo* results demonstrated that the synthesized MPN inhibits glycolysis and mitochondrial metabolism which significantly induced antitumor effects and reduced the production of immunosuppressive metabolites. Furthermore, dual metabolism inhibition induces immunogenic cell death (ICD) due to the enhancement of oxidative stress and starvation-induced autophagy which leads to dendritic cell maturation.
- These findings highlight the potential of combining metabolic therapy with immunotherapy as a novel strategy to enhance antitumor immunity and overcome the limitations of current cancer treatments.

FUNDING SOURCE

4D바이오융합소재 산업화센터 2021R1A6A1A03046418

RESEARCH SCHEME

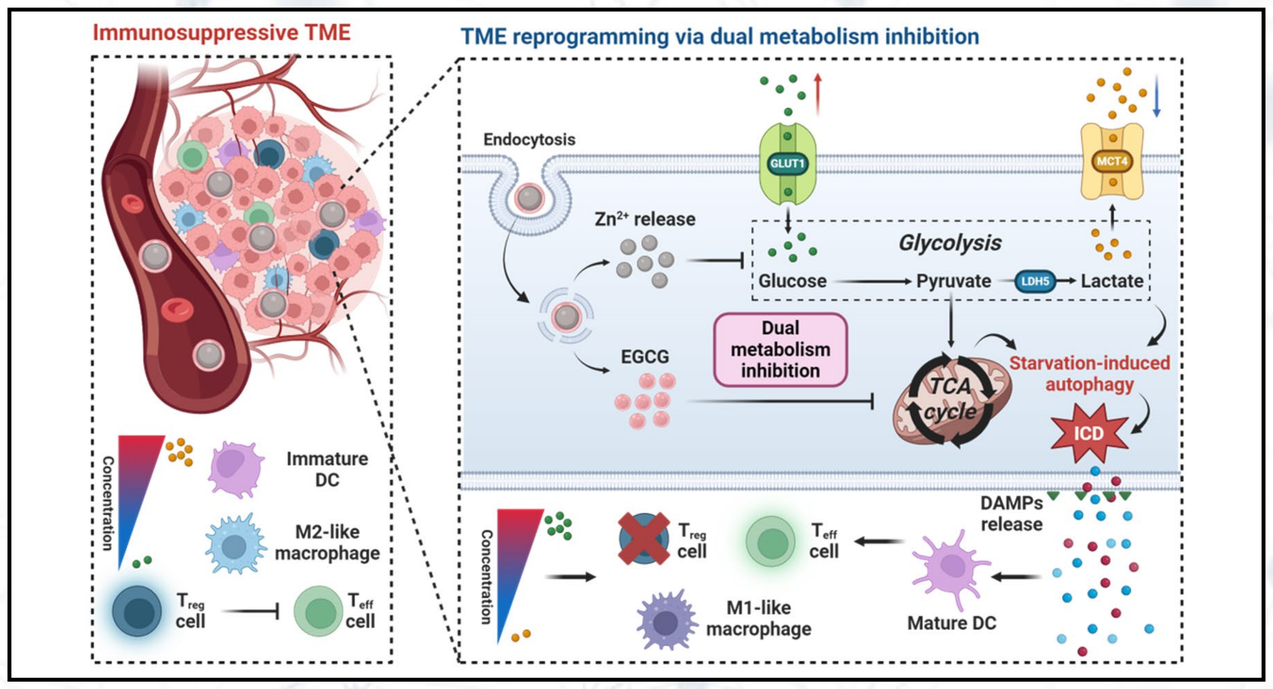

EXPERIMENTAL RESULTS

1. Synthetic method and physical characterization of ZnO-EGCG

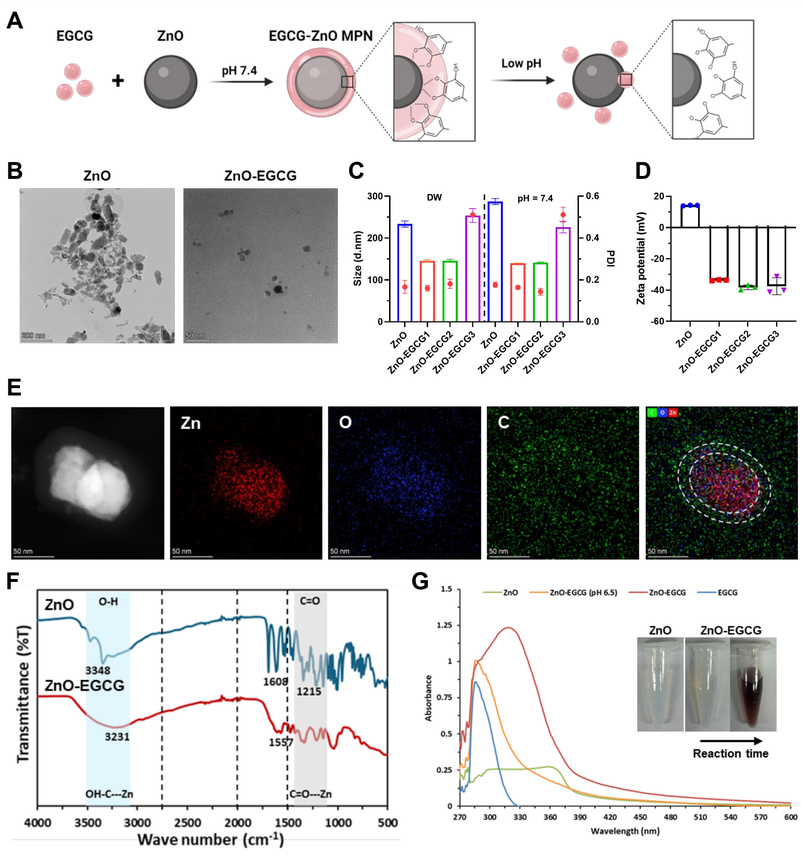

Figure 1. (A) Synthetic procedure and principle of phenolic coating on metal surfaces. (B) TEM image of ZnO and ZnO-EGCG. (C) Size and (D) zeta potential depending on EGCG coating concentration (mg·mL-1). (E) EDS mapping of ZnO-EGCG for elemental analysis.. (F) FT-IR spectra for confirmation of coordination interaction. (F) UV-vis absorption spectra showing pH-responsiveness and image showing color change after reaction.

2. Cytotoxicity and apoptosis inducing ability (*in vitro*)

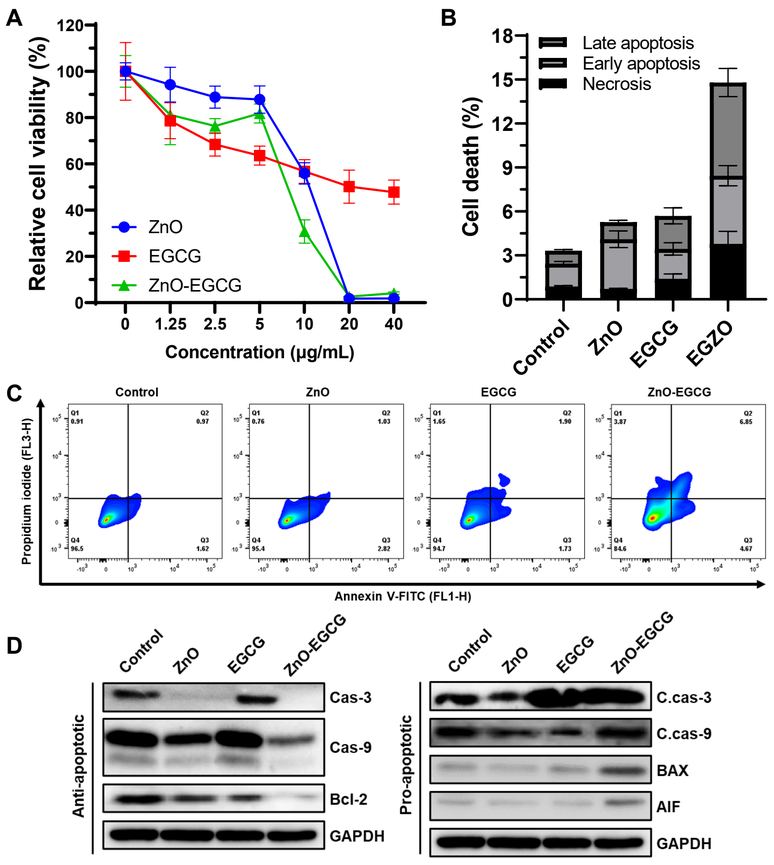

Figure 2. (A) Cytotoxicity against MC38 cell line. (B) Quantitative analysis of apoptotic cells. (C) Histograms of apoptosis induction. (D) Western blot of anti-apoptotic and pro-apoptotic proteins.

3. Glycolysis inhibition leading to tumor microenvironment reprogramming (*in vitro*)

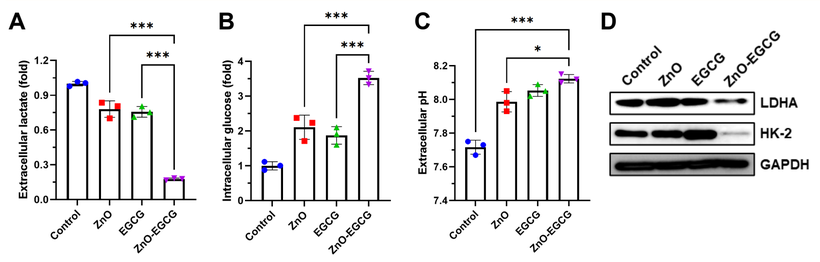

Figure 3. Relative concentration of (A) extracellular lactate and (B) glucose. (C) Extracellular pH measurement for TME analysis. (D) Western blot of glycolysis-related proteins.

4. Mitochondria disruption for dual metabolism inhibition (*in vitro*)

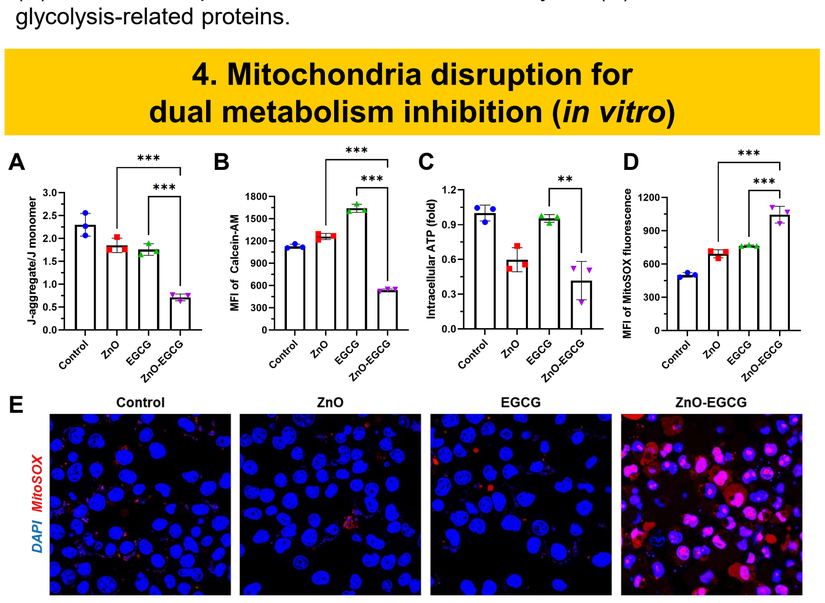

Figure 4. (A) MFI of JC-1 aggregate/monomer indicating mitochondrial membrane potential. (B) MFI of Calcein-AM indicating mitochondrial membrane permeability. (C) Relative intracellular ATP indicating overall metabolic ability of cancer cells. (D) MFI and (E) CLSM images of mitochondrial superoxide release.

5. Immunogenic cell death induction by severe starvation conditions (*in vitro*)

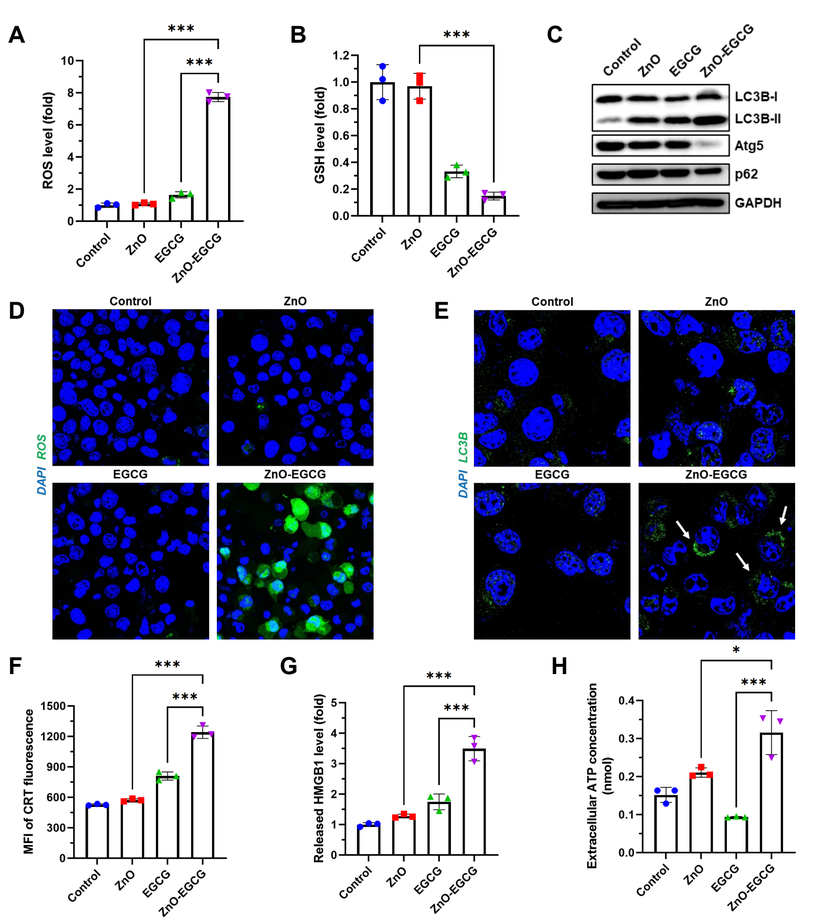

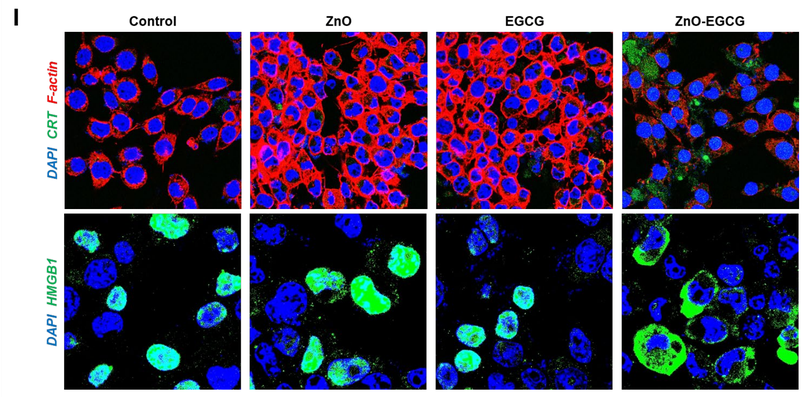

Figure 5. (A) MFI and (D) CLSM images of ROS release and (B) GSH levels indicating oxidative stress. (C) Western blot of autophagy-related proteins. (E) CLSM images of autophagic vesicles. (F, I) CRT exposure, (G, I) HMGB1 and (H) ATP release indicated ICD induction.

6. ICD induction leads to dendritic cell maturation (*in vitro*)

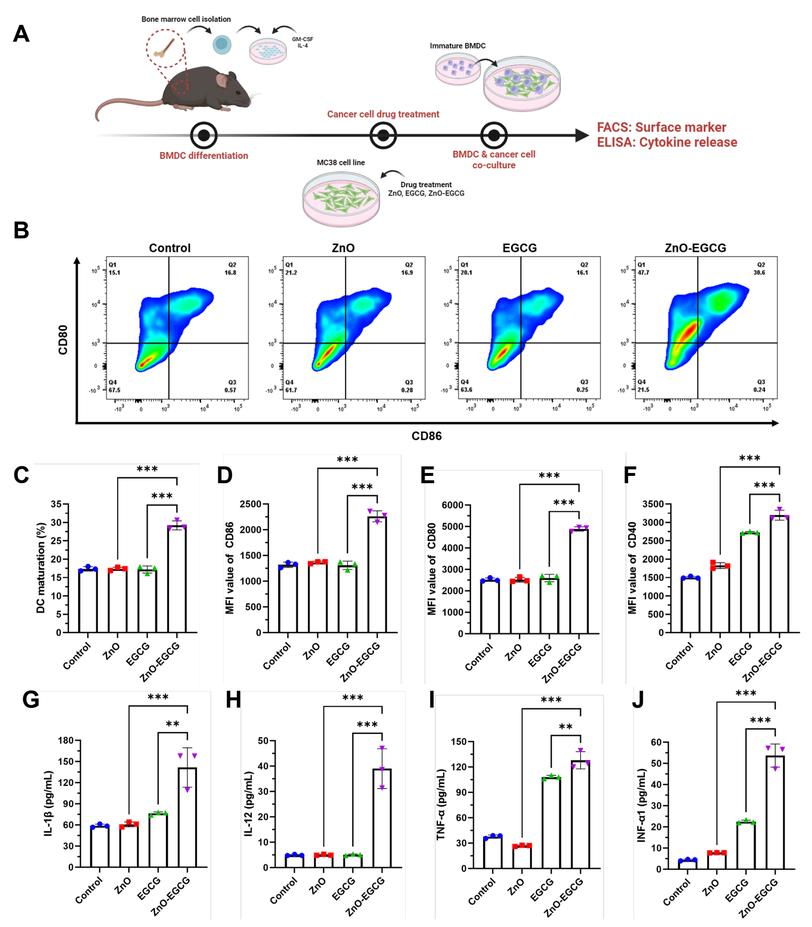

Figure 6. (A) Experimental procedure of BMDC maturation study. (B) Histograms of CD86 and CD80 expressing DCs. (C-F) Surface markers and (G-J) quantification of cytokine release indicating DC maturation.

7. Anticancer efficacy and ICD induction (*in vivo*)

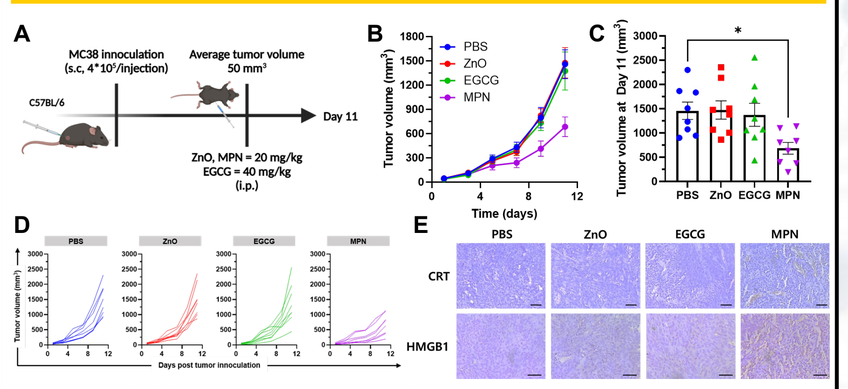

Figure 7. (A) Schematic illustration of dosing schedule. (B) Average and (D) individual tumor growth curves. (C) Tumor volume at day 11. (D) IHC analysis visualizing ICD markers after one day post-administration.